ATOMISTIC STUDIES OF DISLOCATION GLIDE IN γ-TiAl

R. Porizek*, S. Znam*, D. Nguyen-Manh**, V. Vitek* and D. G. Pettifor**
*Department of Materials Science and Engineering, University of Pennsylvania, Philadelphia, Pennsylvania, 19104-6272, U.S.A; **Department of Materials, University of Oxford, Parks Road, Oxford OX1 3PH, UK

ABSTRACT

Computer simulation of the core structure and glide of ordinary 1/2<110] dislocations and <101] superdislocations in $L1_0$ TiAl has been performed using the recently constructed Bond-Order Potentials. This description of atomic interactions includes explicitly, within the tight-binding approximation, the most important aspects of the directional bonding, namely d-d, p-p and d-p bonds. The ordinary dislocation in the screw orientation was found to have a non-planar core and, therefore, high Peierls stress. The superdislocation was found to possess in the screw orientation either a planar (glissile) or a non-planar (sessile) core structure. However, the glissile core transforms into the sessile one for certain orientations of the applied stress. This implies a strong asymmetry of the yield stress and the break down of the Schmid law when the plastic flow is mediated by superdislocations. At the same time, this may explain the orientation dependence of the dislocation substructure observed in the single-phase γ-TiAl by electron microscopy.

INTRODUCTION

It is well established that the main deformation modes in γ-TiAl are slip and twinning, both of them operating on the close-packed {111} planes (see, for example, [1, 2]). The slip occurs via two types of dislocations: ordinary dislocations with Burgers vectors 1/2<110] and superdislocations with Burgers vectors <101]. While the underlying crystallography of the $L1_0$ structure is very close to fcc, and the above mentioned deformation modes are akin to those found in fcc materials, the deformation behavior is much more complex. For example, different deformation modes occur in the single phase and lamellar TiAl and their activity is strongly dependent on temperature [1, 3]. Specifically, in the single phase γ-TiAl <101] superdislocations dominate at low temperatures while at high temperatures (above about 800°C) slip by 1/2<110] ordinary dislocations, and also twinning, become controlling deformation modes. In contrast, in the lamellar TiAl twinning and glide of 1/2<110] ordinary dislocations prevail at low temperatures and glide of superdislocations becomes significant only at high temperatures. In single-phase alloys an anomalous increase of the yield stress with increasing temperature was also observed [3, 4]. .

Understanding of these deformation properties can not be achieved in the framework of the standard elastic theory of dislocations since the core phenomena are likely to play an important role, similarly as in bcc metals and a variety of intermetallic compounds (see, for example, [5-7]). For this reason a number of atomistic studies of dislocations in the $L1_0$ TiAl were carried out in recent years. Most of these calculations were performed using central-force many body potentials of the EAM type [8-10] and only very recently the core structure of the ordinary1/2<110] dislocation was studied using an ab initio DFT based method [11]. While calculations employing central-force schemes revealed a number of general features of dislocations that can be expected in the $L1_0$ structure, they obviously neglect the strong covalent and directional bonding that is characteristic for the titanium aluminides, as documented by DFT based calculations [12-16]. This aspect of bonding is, of course, included in DFT based calculations but in this case the number of atoms that can be fully relaxed is limited to about one hundred.

Recently, we have constructed bond-order potentials (BOPs) for the Ti-Al system in which the most important aspects of the directional bonding, specifically d-d, p-p and d-p bonds, are included explicitly within the tight-binding approximation [17, 18]. The primary advantage of this method, which was developed over a number of years [19-21], is that calculations are performed in the real space and a large number of atoms can be employed when simulating extended defects. The constructed BOPs have been tested by a variety of calculations involving large deviations from the ideal $L1_0$ lattice. For dislocation studies the most important are the energies of stacking-fault like defects. They are for the anti-phase boundary (APB) 545mJm^{-2}, for the complex stacking fault (CSF) 412mJm^{-2} and for the superlattice intrinsic stacking fault (SISF) 140mJm^{-2}. These values

agree well with those found by DFT based calculations [11, 22, 23]. Importantly, the relatively high energy of the SISF is reproduced correctly while for central forces a too low value is usually obtained since it is determined by the interaction of third and other more distant neighbors.

In this paper we present results of atomistic simulations of the core structure and glide of the ordinary screw 1/2<110] dislocation and the screw <101] superdislocation. These calculations show, in agreement with the ab initio study of Woodward and Rao [11], that the ordinary dislocation has a non-planar core and the associated Peierls stress is high. The superdislocation may possess two alternate structures, one planar and the other non-planar. The latter is sessile but the former has a relatively low Peierls stress and is glissile. However, for certain orientations of the applied stress, it transforms into the sessile form, which implies a strong asymmetry of the yield stress and break down of the Schmid law. Furthermore, this behavior may explain the observed dependence of the dislocation substructure in the single-phase γ-TiAl on the orientation of applied stress [24].

1/2<110] ORDINARY DISLOCATION

Atomistic modeling of the dislocation was performed as follows. The slab of the $L1_0$ TiAl structure was first constructed composed of two $(1\bar{1}0)$ planes (one period in the $[1\bar{1}0]$ direction) and the screw dislocation with the Burgers vector $1/2[1\bar{1}0]$ introduced by assigning to all the atoms displacements evaluated in accordance with the anisotropic elastic field of this dislocation in an infinite elastic body. During the calculation periodic boundary conditions were applied in the direction of the dislocation line so that the corresponding block of atoms was effectively infinite in this direction. The block was then divided into an inner part in which the atoms were relaxed, and an outer part in which the atoms were kept displaced in accordance with the elastic field of the dislocation. A molecular statics method of minimizing the energy of the system was employed in the relaxation calculations and the relaxation was always terminated when the force on any atom was smaller than 10^{-2}eV/Å, unless the dislocation began to move. When applying an external stress the elastic displacement field corresponding to this stress was evaluated using anisotropic elasticity and superimposed on the dislocation displacement field for the atoms in both the inner and outer regions. The relaxation then proceeded as in the non-stressed case.

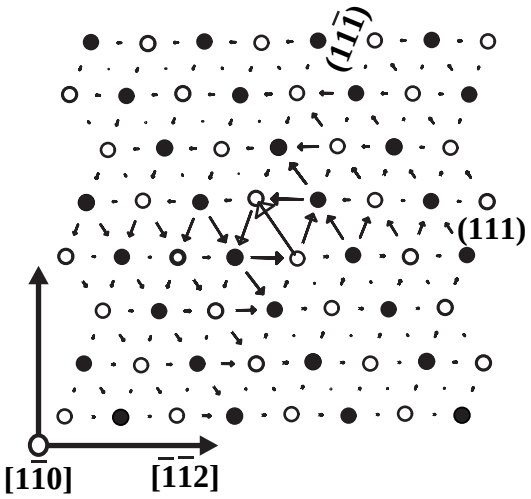

Fig. 1. Differential displacement map of the ordinary $1/2[1\bar{1}0]$ screw dislocation

Study of the effect of an applied stress always started with the fully relaxed core structure of the dislocation. The stress was then increased incrementally and full relaxation carried out at every step until the dislocation started to move. This stress level was identified with the critical stress needed for the dislocation glide at 0^{o}K.

The relaxed structure of the $1/2[1\bar{1}0]$ screw dislocation is shown in Fig. 1 using the method of differential displacements (see e. g. [6]). The atomic arrangement is shown in the projection perpendicular to the direction of the dislocation line and circles represent atoms within one period without distinguishing their positions in two successive $(1\bar{1}0)$ planes. The open and filled circles represent the positions of Al and Ti atoms, respectively. The screw component (in the $[1\bar{1}0]$ direction) of the relative displacement of the neighboring atoms, produced by the dislocation, is depicted as an arrow between them. The length of the arrows is proportional to the magnitude of this displacement. It is seen that the core of this dislocation is spread symmetrically into two {111} planes, specifically (111) and $(11\bar{1})$. The same core structure has also been found in the ab initio

calculations of Woodward and Rao [11]. In principle, a planar configuration corresponding to the dissociation into Shockley partials separated by the CSF ($1/2[1\bar{1}0] = 1/6[1\bar{2}1] + 1/6[2\bar{1}\bar{1}]$) could exist. Such configuration has, indeed, been found as an alternative to the non-planar configuration in several studies employing central-force potentials [8-10]. However, in the present calculations the non-planar core is the only structure found. The reason is, apparently, the high energy of the CSF. Using the anisotropic elastic theory of singular dislocations, the width of the splitting of the $1/2[1\bar{1}0]$ screw dislocation into Shockley partials for the CSF energy of $412 mJm^{-2}$ would be smaller than one lattice spacing.

The result of the application of pure shear stress in the $[1\bar{1}0]$ direction in the $(11\bar{1})$ plane is shown in Fig. 2. The dislocation core first partially constricts in both (111) and $(11\bar{1})$ plane and the dislocations starts to move along the $(11\bar{1})$ plane at the applied stress of $0.04C_{44}$. This magnitude of the critical resolved shear stress (CRSS) in the slip plane (Peierls stress), is typical for non-planar cores. Similar values were found for screw dislocations in bcc metals that also possess cores of this type [25-27]. Application of the shear stress on different planes of the $[1\bar{1}0]$ zone always induces glide along either (111) or $(11\bar{1})$ plane, depending on the Schmid factor.

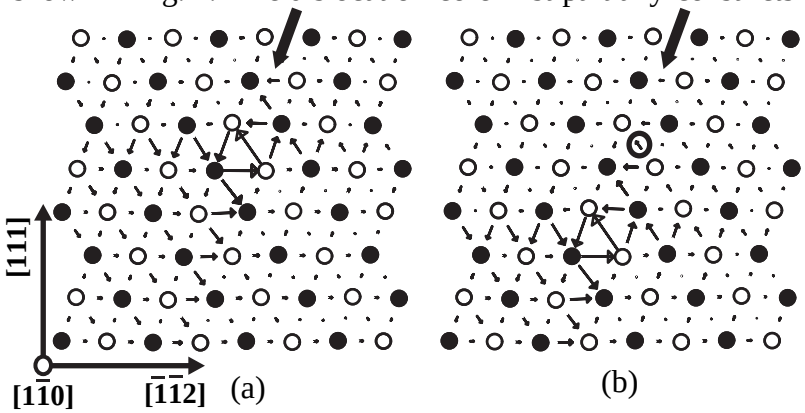

Fig. 2. Effect of the shear stress applied in the $(11\bar{1})$ plane on the $1/2[1\bar{1}0]$ screw dislocation; the arrow shows the direction of the corresponding Peach-Koehler force. (a) The core structure at the stress somewhat lower than the Peierls stress. (b) Movement of the dislocation; the large open circle marks the original position of the dislocation.

<101] SUPERDISLOCATION

Atomistic modeling of the $[10\bar{1}]$ superdislocation in the screw orientation was carried out in the same way as in the case of the ordinary dislocation. However, as discussed below, this dislocations splits into well defined partials and thus the elastic displacement field was adjusted accordingly, i. e. in the fully relaxed structure it was identified with the anisotropic elastic field of the corresponding configuration of the partial dislocations. These calculations revealed two distinct configurations shown in Figs. 3a and b. In these figures the atomic arrangement is again shown in the projection perpendicular to the direction of the dislocation line and circles represent atoms within one period without distinguishing their positions in four successive $(10\bar{1})$ planes. However, unlike in the case of the ordinary dislocation, Al and Ti atoms are also not distinguished since Al and Ti alternate in the rows parallel to the $[10\bar{1}]$ direction. The screw component (in the $[10\bar{1}]$ direction) of the relative displacement of the neighboring atoms, produced by the dislocation, is again depicted as an arrow between them and the regions where such displacements are constant correspond to metastable stacking-fault like defects.

The detailed analysis of the planar structure shown in Fig. 3a reveals that it corresponds to the dissociation according to the reaction

$$[10\bar{1}] = \tfrac{1}{6}[11\bar{2}] + \tfrac{1}{2}[10\bar{1}] + \tfrac{1}{6}[2\bar{1}\bar{1}] \qquad (1a)$$

with the SISF between the partials $\frac{1}{6}[11\bar{2}]$ and $\frac{1}{2}[10\bar{1}]$ and the CSF between the partials $\frac{1}{2}[10\bar{1}]$ and $\frac{1}{6}[2\bar{1}\bar{1}]$. Using the anisotropic elastic theory of singular dislocations and the energies of

SISF and CSF determined in the framework of the BOP for TiAl, the width of the SISF in this splitting is 9.6*a* and the width of the CSF 2.75*a* (*a* is the lattice spacing). The widths of the stacking faults in Fig. 3a are, indeed, close to these values.

The non-planar configuration, shown in Fig. 3b, corresponds to the dissociation according to the reaction

$$[10\bar{1}] = \tfrac{1}{6}[11\bar{2}] + \tfrac{1}{3}[20\bar{1}] + \tfrac{1}{6}[1\bar{1}\bar{2}] \qquad (1b)$$

with the SISF on both (111) and $(1\bar{1}1)$ planes. Within the anisotropic elastic theory of singular dislocations and for the energy of the SISF determined using the BOP for TiAl, the width of the SISF is 8.25*a*. This is again close to the width found in the atomistic study. This configuration is akin to the Lommer-Cottrell lock, found in fcc materials. Such locks are immobile and can act as strong obstacles to the dislocations motion. Hence, during plastic deformation superdislocations have to be generated such that their screw parts are in the planar, glissile form, split according to equation (1a). We studied the glide of such screw dislocations under the effect of externally applied shear stress, similarly as in the case of the ordinary dislocation.

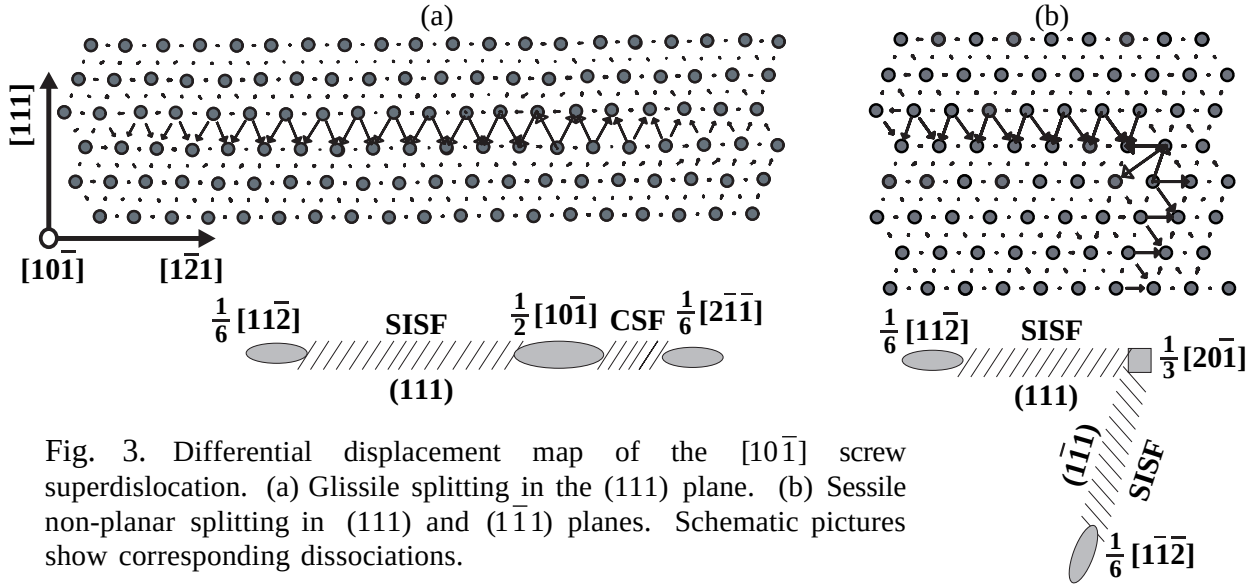

Fig. 3. Differential displacement map of the $[10\bar{1}]$ screw superdislocation. (a) Glissile splitting in the (111) plane. (b) Sessile non-planar splitting in (111) and $(1\bar{1}1)$ planes. Schematic pictures show corresponding dissociations.

When applying the shear stress in the (111) plane in the $[10\bar{1}]$ direction such that the $\frac{1}{6}[11\bar{2}]$ partial bounding the SISF would be leading during the glide, the dislocation configuration always transformed into the non-planar form. The dislocation thus became completely locked. In contrast, when the shear stress was applied such that the $\frac{1}{6}[11\bar{2}]$ partial would be trailing during the glide, the dislocation core structure transformed into that shown in Fig. 4. This configuration is planar, though with the CSF one layer below that of the unstressed state, and starts to move at the stress of $0.006C_{44}$. Obviously, the ability of the dislocation to glide depends strongly on the sense of shearing which is in contrast with the Schmid law.

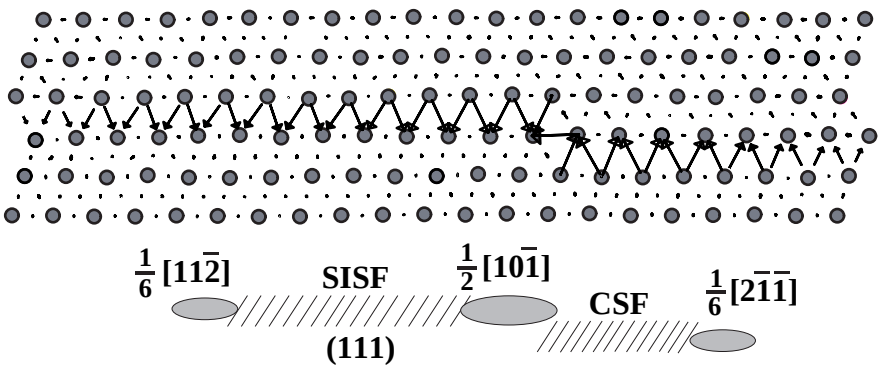

Fig. 4. Effect of the shear stress applied in the (111) plane such that the $1/6[2\bar{1}\bar{1}]$ partial bounding the CSF is leading.

Application of the shear stress on different planes of the [10$\bar{1}$] zone, which corresponds to different orientations of the maximum resolved shear stress plane with respect to the (111) plane, revealed that the locking of the screw dislocation by transformation into the non-planar form is principally controlled by the shear stress in the cross-slip plane (1$\bar{1}$1). If the stress in this plane acts such that the $\frac{1}{6}$[1$\bar{1}\bar{2}$] partial of the splitting (1b) would be pushed further away from the intersection of the (111) and (1$\bar{1}$1) planes, i. e. away from the partial $\frac{1}{3}$[20$\bar{1}$], the locking occurs. In the opposite case the dislocation remains planar. Obviously, when the shear stress is applied in the (111) plane such that the $\frac{1}{6}$[11$\bar{2}$] partial is leading, the $\frac{1}{6}$[1$\bar{1}\bar{2}$] partial of the splitting (1b) would be pushed further away from the partial $\frac{1}{3}$[20$\bar{1}$]. The opposite situation arises when the shear stress in the (111) plane is applied such that the $\frac{1}{6}$[11$\bar{2}$] partial would be trailing.

DISCUSSION

The present results suggest, similarly as the results of recent ab initio calculations [11], that the ordinary 1/2<110] dislocation in the screw orientation possesses a non-planar core, spread symmetrically into two planes of the {111} type. Under the effect of applied stresses, this dislocation always glides on one of these {111} planes, depending on the magnitude of the corresponding Schmid factor. The Peierls stress of this dislocation is high, comparable with that of similarly spread screw dislocations in bcc metals [25-27]. Since the core spreading is very narrow, overcoming of the Peierls barrier can be aided by thermal activation, for example via the formation of pairs of kinks. This implies that when the slip is controlled by ordinary 1/2<110] dislocations the flow stress will be rapidly decreasing with increasing temperature. This is in agreement with the observations that in the single phase γ-TiAl the glide of 1/2<110] ordinary dislocations becomes dominant only at high temperatures [1, 3].

On the other hand, the planar splitting of the screw <101] superdislocation is glissile with significantly lower Peierls stress than that of ordinary dislocations. Indeed, in the single phase γ-TiAl <101] superdislocations dominate at low temperatures [1, 3]. The glissile form of the superdislocations corresponds to the splitting according to equation (1a) and involves both the SISF and CSF. However, the CSF ribbon is only two to three lattice spacings wide and cannot be resolved in TEM weak-beam images. Hence, interpretation of the observed splitting of the [10$\bar{1}$] superdislocation [24, 28] as dissociation into two partials according to the reaction

$$[10\bar{1}] = \tfrac{1}{6}[11\bar{2}] + \tfrac{1}{6}[5\bar{1}\bar{4}], \qquad (2)$$

with the SISF between them, is consistent with the results of the present atomistic study. However, the dissociation according to the reaction

$$[10\bar{1}] = \tfrac{1}{6}[11\bar{2}] + \tfrac{1}{6}[2\bar{1}\bar{1}] + \tfrac{1}{2}[10\bar{1}] \qquad (3)$$

with the SISF between the partials $\frac{1}{6}$[11$\bar{2}$] and $\frac{1}{6}$[2$\bar{1}\bar{1}$] and APB between the partials $\frac{1}{6}$[2$\bar{1}\bar{1}$] and $\frac{1}{2}$[10$\bar{1}$], suggested by several observations [29, 30], was found to be unstable in the present calculations. The reason is, presumably, that the energy of the CSF is appreciably lower than that of the APB.

However, in the screw orientation the [10$\bar{1}$] superdislocation may also assume a sessile form, corresponding to the splitting according to equation (1b). This plays an important role in the glide of screw superdislocations which was found to be very different depending on whether the $\frac{1}{6}$[11$\bar{2}$] partial bounding the SISF is leading or trailing, and/or whether the applied stress extends or contracts the possible splitting into the (1$\bar{1}$1) plane. In the former case the glissile superdislocation transforms in the screw orientation into the sessile one, while in the latter case it remains glissile. The sessile screw segments of superdislocations will act as obstacles for dislocation motion and thus it can be expected that the yield stress will be higher when the partial bounding the SISF is leading. This has, indeed, been observed in [3, 31]. Furthermore, Veyssiere and co-workers [24,

28] found frequent formation of faulted dipoles when the partial bounding the SISF is leading but not when it is trailing during glide. The present atomistic study provides a physical justification for the formation of sessile segments of superdislocation during their glide when the partial bounding the SISF is leading. Such segments are a necessary precursor for the formation of the faulted dipoles as discussed in [24]. A more detailed mechanism of the formation of such dipoles when sessile segments of the type predicted in the present study occur, will be discussed elsewhere.

ACKNOWLEDGMENTS

This research was supported in part (RP, SZ and VV) by the National Science Foundation grant no. DMR99-81023.

REFERENCES

1. M. Yamaguchi, H. Inui, S. Yokoshima, K. Kishida and D. R. Johnson, *Mat. Sci. Eng. A* **213**, 25 (1996).
2. S. Sriram, V. K. Vasudevan and D. Dimiduk, *High-Temperature Ordered Intermetallic Alloys VI*, edited by J. A. Horton, I. Baker, S. Hanada, R. D. Noebe and D. S. Schwartz (Pittsburgh, Materials Research Society), Vol. 364, p. 647 (1999).
3. H. Inui, M. Matsumuro, D. H. Wu and M. Yamaguchi, *Philos. Mag. A* **75**, 395 (1997).
4. T. Kawabata, T. Kanai and O. Izumi, *Acta Metall.* **33**, 1355 (1985).
5. M. S. Duesbery, *Dislocations in Solids*, edited by F. R. N. Nabarro (Amsterdam, Elsevier), Vol. 8, p. 67 (1989).
6. V. Vitek, *Prog. Mater. Sci.* **36**, 1 (1992).
7. V. Vitek, *Intermetallics* **6**, 579 (1998).
8. A. Girshick and V. Vitek, *High-Temperature Ordered Intermetallic Alloys VI*, edited by J. Horton, I. Baker, S. Hanada, R. D. Noebe and D. Schwartz (Pittsburgh, Materials Research Society), Vol. 364, p. 145 (1995).
9. J. P. Simmons, S. I. Rao and D. M. Dimiduk, *Philos. Mag. A* **75**, 1299 (1997).
10. J. Panova and D. Farkas, *Philos. Mag. A* **78**, 389 (1998).
11. C. Woodward and S. I. Rao, *Philos. Mag. A*, in press (2003).
12. Y. Song, S. P. Tang, J. H. Xu, O. N. Mryasov, A. J. Freeman, C. Woodward and D. M. Dimiduk, *Philos. Mag. B* **70**, 987 (1994).
13. N. Nguyen-Manh, A. M. Bratkovsky and D. G. Pettifor, *Phil. Trans. Roy. Soc. London A* **351**, 529 (1995).
14. J. Zou, C. L. Fu and M. H. Yoo, *Intermetallics* **3**, 265 (1995).
15. D. Nguyen-Manh and D. G. Pettifor, *Intermetallics* **7**, 1095 (1999).
16. D. Nguyen-Manh and D. G. Pettifor, *Gamma Titanium Aluminides*, edited by Y. W. Kim (Pittsburgh, TMS), p. 175 (1999).
17. S. Znam, Philadelphia, University of Pennsylvania, (2001).
18. S. Znam, D. Nguyen-Manh, D. G. Pettifor and V. Vitek, *Philos. Mag. A*, in press (2003).
19. D. G. Pettifor, *Phys. Rev. Lett.* **63**, 2480 (1989).
20. A. P. Horsfield, A. M. Bratkovsky, M. Fearn, D. G. Pettifor and M. Aoki, *Phys. Rev. B* **53**, 1656, 12694 (1996).
21. D. G. Pettifor, I. I. Oleinik, D. Nguyen-Manh and V. Vitek, *Comp. Mat. Sci.* **23**, 33 (2002).
22. V. Vitek, K. Ito, R. Siegl and S. Znam, *Mat. Sci. Eng. A* **240**, 752 (1997).
23. J. Ehmann and M. Fähnle, *Philos. Mag. A* **77**, 701 (1998).
24. F. Gregori and P. Veyssiere, *Philos. Mag. A* **80**, 2913, 2933 (2000).
25. K. Ito and V. Vitek, *Philos. Mag. A* **81**, 1387 (2001).
26. S. I. Rao and C. Woodward, *Philos. Mag. A* **81**, 1317 (2001).
27. C. Woodward and S. I. Rao, *Philos. Mag. A* **81**, 1305 (2001).
28. P. Veyssiere, Y.-L. Chiu and F. Gregori, *Defect Properties and Related Phenomena in Intermetallic Alloys*, edited by E. P. George, M. J. Mills, H. Inui and G. Eggeler, this volume (2003).
29. G. Hug, A. Loiseau and P. Veyssiere, *Philos. Mag. A* **57**, 499 (1988).
30. Z. X. Li and S. H. Whang, *Mat. Sci. Eng. A* **152**, 182 (1992).
31. H. Inui and M. Yamaguchi, *Electron Microscopy* **32**,144 (1997).